

Electric field manipulation of particles in leaky dielectric liquids

Z. ROZYNEK^{1,2)}, R. CASTBERG^{3,4)}, A. KALICKA¹⁾,
P. JANKOWSKI¹⁾, P. GARSTECKI¹⁾

¹⁾*Institute of Physical Chemistry
Polish Academy of Sciences
Kasprzaka 44/52
01-224 Warsaw, Poland
e-mails: zbigniew.rozynek@gmail.com, garst@ichf.edu.pl*

²⁾*Department of Physics
Norwegian University of Science and Technology
Hoegskoleringen 5
N-7491 Trondheim, Norway*

³⁾*Department of Physics
University of Oslo
P.O. Box 1048
NO-0316, Oslo, Norway*

⁴⁾*DNV GL Strategic Research and Innovation
NO-1322, Høvik, Norway*

PATCHY COLLOIDAL CAPSULES, i.e., hollow structures with permeable heterogeneous surfaces, possess advantageous properties when compared with their homogenous counterparts. For example, owing to specific interactions between patches they can self-assemble into complex structures to form functional materials. Fabrication of patchy colloidal capsules has long been theorized by scientists able to design different models, but the actual production of them remains a challenge. Here, we demonstrate how to manipulate colloidal particles on a surface of a droplet with electric fields. We present three examples of patchy structures formed via electrohydrodynamic microflows and electro-coalescence. In addition, we show electro-orientation of patchy capsules composed of both nonconductive polymeric particles and conductive silver coated particles. Finally, we discuss the importance of an appropriate selection of oils and particles.

Key words: patchy structures, guided-assembly, electrohydrodynamics, electro-orientation.

1. Introduction

The patterns of flow induced by electric fields on a surface of a droplet were first observed and described nearly half a century ago [1]. Still, it has only recently been demonstrated that these flows can be used to carry and manipulate colloidal particles located on the surface of a droplet [2]. As a result, the particles assemble into clusters and, interestingly, the size, shape and location of these clusters are strongly affected by the frequency and amplitude of the electric field. Depending on electric field (E -field) strength and concentration of colloidal particles, the clusters may either remain in motion (e.g., spinning domains [2, 3]) or form stagnant patterns [4]. The latter are more relevant to fabricating novel materials (e.g., heterogeneous capsules [4]). We previously demonstrated fabrication of highly ordered jammed colloidal capsules of various shapes, including Janus and patchy capsules, by electro-coalescing two or more droplets with prearranged particles [4].

Heterogeneous colloidal capsules (comprising of two micro- or nano-particle shells, each characterized by different properties) offer a few advantages when compared to their homogenous counterparts commonly prepared by emulsification. For example, owing to specific interactions between patches they can self-assemble into complex structures (similarly to patchy particles) to form different porous two- and three-dimensional structures [5], e.g., scaffolds [6]. Self-assembly of the supra-structures can be effectively steered by both the shape of the shell and the distribution and type of the patches on their surfaces [7].

Colloidal capsules can be also used as carriers for drug molecules [8], enzymes [9] or dyes [10]. Patchy colloidal capsules have potential in making smart delivery systems, for example, if a shell is designed to exhibit self-propulsion. We foresee, this can be achieved if a specific patch of the shell is composed of Janus colloidal particles coated on one side with active substances that provide power for a capsule motor, e.g., by catalytic decomposition [11]. These micro-vehicles could also be steered. In the presence of external fields (magnetic or electric), the Janus capsules may undergo rotation similarly to Janus particles [12] or – as we demonstrate here – electro-orientation.

The surface density of colloidal particles determines the permeability of the capsule. Recently, we showed how to control the packing density (to a certain degree) via electro-deformation of a droplet induced by slowly alternating E -fields [13]. The permeability of the capsule can be also actively controlled, for example, when pH-responsive colloidal particles are used to form a shell [14].

Properties of patchy shells and their application have long been theorized by scientists able to design different models [15, 16], but the actual production of them remains a challenge. Here, we show fabrication of patchy structures (including patchy ribbons and shells) with the use of electro-hydrodynamic (EHD)

flows. The layout of the present work is as follows. Firstly, we discuss the behavior of droplets subjected to electric fields in Section 2.1, followed by deformation dynamics and charge build-up in ‘leaky dielectric’ liquids in Section 2.2. The mechanism of generation of microflows is described in Section 2.3 and the application of the fluid motion for manipulating of surface particles is presented in Section 2.4. In Section 2.5 we discuss the importance of an appropriate selection of oils and particles. Conclusions are presented at the end in Section 3.

2. Results

2.1. Dielectric versus ‘leaky dielectric’ surrounding liquids

We will briefly discuss the behavior of droplets subjected to E -fields. An external E -field applied to a droplet surrounded by a dielectric medium, deforms the droplet to a prolate geometry, i.e., both the direct current (DC) and alternating current (AC) E -fields stretch droplets along the direction of the E -field. The deformation can be quantified by a parameter

$$D = \frac{x_{\parallel} - x_{\perp}}{x_{\parallel} + x_{\perp}},$$

where x_{\parallel} and x_{\perp} are the lengths of the droplet in the direction parallel and perpendicular to the electric field. The values of the dielectric constants (ε_d – droplet, ε_s – surrounding medium) together with the strength of the E -field determine the magnitude of D . The capillary pressure acts perpendicular to the surface of the droplet to maintain the spherical shape. The deformation D is thus inversely proportional to the surface tension between the liquids γ and can be reformulated as:

$$(2.1) \quad D = \frac{9}{16} \frac{\varepsilon_s \varepsilon_0 a E^2}{\gamma} \left(\frac{\varepsilon_d - \varepsilon_s}{\varepsilon_d + 2\varepsilon_s} \right)^2 > 0 \quad \text{for a dielectric droplet}$$

$$(2.2) \quad D = \frac{9}{16} \frac{\varepsilon_s \varepsilon_0 a E^2}{\gamma} > 0 \quad \text{for a conductive droplet,}$$

where a is the radius of undeformed droplet, and ε_0 is the vacuum permittivity [17]. Interestingly, irrespectively on the sign of $\varepsilon_d - \varepsilon_s$, the system lowers its energy in the presence of the E -field by elongating the droplet along the field lines, thus the deformation is always positive.

Generally, the two aforementioned models are accurate for small deformations and under the assumption that the surrounding medium is dielectric (electrically non-conductive liquid). In Fig. 1 a droplet of silicone oil (Down Corning 200/50 cSt, specific density of 0.962 g/cm³ at 25°C, electric conductivity ~ 3 –5 pS/m, relative permittivity 2.1) with a radius of approx. 1.7 mm is immersed in castor oil (Sigma-Aldrich 83912, specific density of 0.961 g/cm³ at

25°C, electric conductivity $\sim 40\text{--}45$ pS/m, relative permittivity 4.7 and viscosity around 700 cSt). A 100 Hz external AC E -field of 200 V/mm applied in the horizontal direction deforms the droplet that acquires a prolate shape (see Fig. 1b). The deformation D is ~ 0.01 (for Fig. 1b), a value that coincides well with a theoretical prediction given by Eq. 2.1, assuming the surface tension is 5 mN/m.

Application of a DC E -field of similar strength results in a different deformation of the droplet. As shown in Fig. 1c, the droplet deforms in the direction perpendicular to the E -field lines and becomes oblate ($D < 0$). This behavior is not predicted by the dielectric models presented above. TAYLOR [1] realized that the surrounding fluid could no longer be viewed as an insulator, i.e., even in very pure oils there are mobile charges (ions) that are able to reach the interface of the droplet. The two aforementioned oils should hence be considered as ‘leaky dielectric’ fluids (weakly electrically conductive liquids).

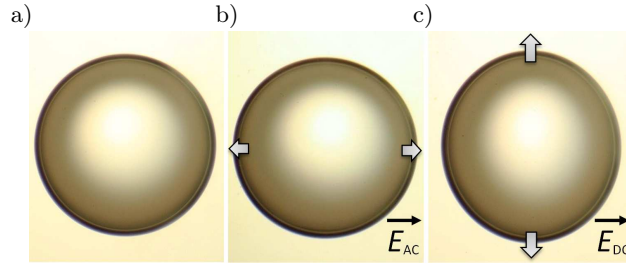


FIG. 1. A silicone oil droplet of radius 1.7 mm immersed in castor oil. Panel (a) shows the situation before the E -field is turned on, while panels (b) and (c) illustrate prolate and oblate deformations at steady state after the application of AC (100 Hz) and DC E -fields of approx. 200 V/mm, respectively. The E -field direction is horizontal.

Taylor proposed a model [1] that describes the behavior of droplets deformed by a DC E -field. The leaky dielectric model includes the contributions from the electrical conductivities and viscosities of both liquids, and describes the deformation as [18]:

$$(2.3) \quad D = \frac{9}{16} \frac{\varepsilon_s \varepsilon_0 a E^2}{\gamma} \frac{\Phi}{(2 + R)^2}$$

and

$$(2.4) \quad \Phi = R^2 + 1 - 2G + \frac{3}{5}(R - G) \frac{2 + 3\lambda}{1 + \lambda},$$

where $R = \sigma_d/\sigma_s$ is the ratio of conductivities, $G = \varepsilon_d/\varepsilon_s$ is the ratio of dielectric constants, and $\lambda = \eta_d/\eta_s$ is the ratio of viscosities. Within this model, the deformation can accept both negative and positive values. Prolate shapes ($D > 0$) are predicted for $\Phi > 1$, and oblate shapes when $\Phi < 1$. The value of D for

the droplet shown in Fig. 1c is ~ -0.03 , which agrees well with the theoretical prediction given by Eqs. 2.3 and 2.4. It is important to note that Eqs. 2.3 and 2.4 for D describe drop deformation in a DC E -field. However, those equations still hold for an AC E -field that has an oscillation period much longer than the time needed for charges to accumulate on the surface of a droplet, i.e., $f < 1/\tau_{\text{MW}}$.

2.2. Deformation dynamics and charge build-up in ‘leaky dielectric’ liquids

If there is a mismatch in conductivities between the surrounding liquid and a droplet, mobile ions will start building up at the outer surface of the droplet. The conductivity of castor oil (outer phase) is approx. 10 times larger than the conductivity of silicone oil. The Maxwell–Wagner polarization time [19] predicts the interval needed for accumulation of charge at the interfaces. This time does not depend on the strength of the E -field:

$$(2.5) \quad \tau_{\text{MW}} = \frac{\varepsilon_d + 2\varepsilon_s}{\sigma_d + 2\sigma_s} \varepsilon_0, \quad \text{here } \tau_{\text{MW}} \approx 1.2 \text{ s.}$$

The time it takes for a droplet to deform due to the EHD flow and reach an equilibrium shape is determined by the viscosities of both fluids and by the strengths of the applied E -field [20]:

$$(2.6) \quad \tau_{\text{EHD}} = \frac{\eta_s}{\varepsilon_s \varepsilon_0 E^2} \left(1 + \frac{\eta_d}{\eta_s} \right).$$

Figure 2a presents the measurements of the deformation of a 2.2 mm droplet as a function of both the strength of the DC E -field and of the time from turning

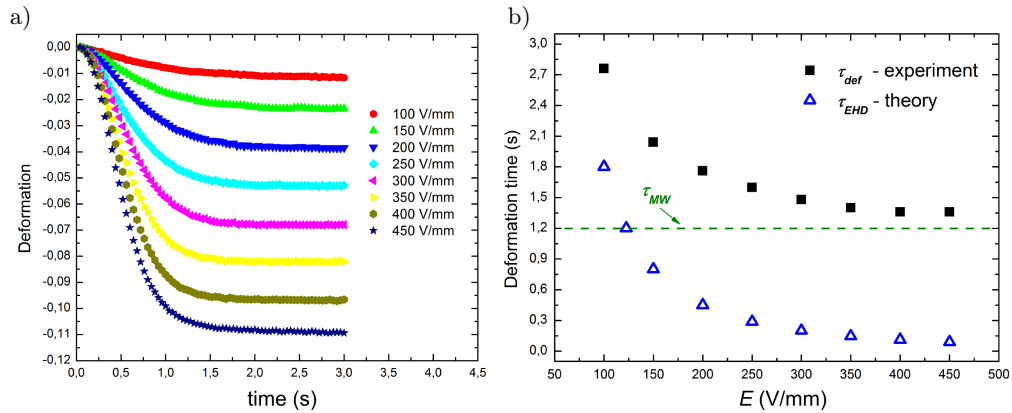


FIG. 2. a) Deformation dynamics of a silicone oil droplet of radius 2.2 mm immersed in castor oil at different DC E -field strengths. b) At E -fields above 250 V/mm the characteristic deformation time τ_{def} approaches the theoretical value of the Maxwell–Wagner time τ_{MW} (around 1.2 s), whereas for lower E -fields the significance of τ_{EHD} rises, thus τ_{def} becomes strongly E -field-dependent. The theoretical values of τ_{EHD} are marked as open triangles.

the DC E -field on. We define the deformation time τ_{def} as the interval after which D reaches the arbitrarily set threshold of 97% of its peak value. Figure 2b shows τ_{def} plotted against the strength of the DC E -field (filled squares). At DC E -fields above 250 V/mm the characteristic deformation time approaches the theoretical value of the Maxwell–Wagner time, whereas for lower DC E -fields it becomes predominantly dependent on τ_{def} , thus strongly E -field-dependent. The theoretical values of τ_{def} are marked as open triangles.

The estimated value for the charge build-up time (from Eq. 2.5) is approx. 1.2 s, and this sets the critical frequency of around 0.8 Hz for the applied AC E -fields, above which the charge build-up will be suppressed. The E -field strength has its upper limit as well, above which a deformed droplet starts rotating in a manner resembling the Quincke rotation [21]. In our system, for a droplet size of around 2 mm, this critical E -field strength is of about 700 V/mm, and is roughly two times higher from what it would be expected from the Quincke theory for a rigid sphere possessing similar dielectric parameters as the silicone oil droplet. At very high fields the droplet breaks up [20].

2.3. Electric-field-induced hydrodynamic flows

Mobile charges that buildup at the interface of the droplet are distributed around the entire droplet except for the ‘electric equator’. The force on the charges acts on the droplet in the direction of the E -field lines. There are only two points on the droplet (its ‘electric poles’) where the electric force is oriented entirely along the normal to the surface. Everywhere else the electric force has two components, namely normal and tangential components. While the normal component is balanced by the surface tension, the tangential component is balanced by the viscous shear stress, i.e., the tangential component of the electric force sets the fluids in motion [1].

The Taylor electrohydrodynamic model describes both the direction and magnitude of the flow. The direction of flow is from the electric poles towards the electric equator. Experimentally we observed similar flow patterns by tracing microparticles. Figure 3a shows the observed flow patterns. The arrows indicate the direction of movement of several tracer particles. Figure 3b shows a different droplet with several tracer particles capillary bound to the liquid interface. After the application of an electric field, the surface particles are carried by the EHD flows towards the electric equator, as indicated by the blue arrows. Figures 3a and 3b were composed by stacking several images captured over a period of around 4 and 3 seconds, respectively. We consider the microparticles as pure traces, since we observed no direct interaction of the electric field with them (e.g., no electrophoretic or dielectrophoretic motion). The gravity direction is vertical, while the E -field of around 200 V/mm is applied in the horizontal direction.

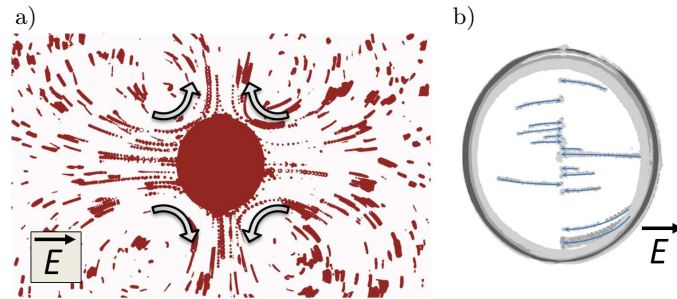


FIG. 3. Experimentally observed hydrodynamic streamlines: a) outside the droplet and b) on the surface of droplet. The arrows indicate the direction of movement of several tracer particles. The size of each droplet is about 3 mm. The E -field of 200 V/mm applied in the horizontal direction.

Surprisingly, the flow induced by the electric-field (both inside and outside the droplet) has barely been studied in the context of particle manipulation and of guided-assembly. In the next subsections, we show examples of how non-conductive particles can be assembled into simple structures.

2.4. Particle manipulation on the surfaces of droplets

EHD flows can be used to arrange colloidal particles on the surface of a droplet. When using silicone and castor oils (with the same parameters as presented before) with moderate E -fields, (up to around 350 V/mm the liquid flows in the direction from the electric poles towards the electric equator (as indicated in Fig. 3). If non-conductive particles with similar dielectric properties as those of the oils are randomly dispersed on the surface of the droplet, the flow will carry these particles towards the electric equator. At this position, the silicone oil moves away from the interface, into the bulk of the droplet, yet the particles are held at the interface by capillary forces. As a result, the particles assemble into a ‘ribbon-like’ structure [4] at the surface of the droplet. The width of the ribbon primarily depends on the concentration (surface density) of particles at the interface. The dynamics of assembly are determined mainly by the viscosity of both liquids and on the strength of the E -field.

It is also possible to form more complex ribbon-like structures by coalescing two (as shown in Fig. 4) or more droplets, each containing different particles. In the example below we demonstrate the method of fabricating a two-stripped ribbon and a ribbon that is composed of two half rings of different materials.

We start the experiment with two droplets, one containing red and one with green polyethylene (UVPMS 45–53 μm , Cospheric LLC) particles randomly dispersed on their surfaces (left panel in Fig. 4). Application of a DC E -field (~ 250 V/mm) causes aggregation of the particles at the equators. At the same

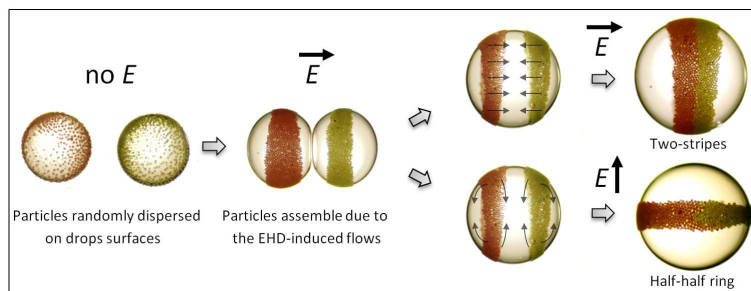


FIG. 4. The process of forming a two-striped ribbon and a ribbon composed of two half rings. Two droplets with red and green PE particles located on the droplets surfaces are brought to close proximity. Due to the EHD flows, the particles assemble at the droplets' electric equator. By coalescing the droplets, a two-striped ribbon is formed (top right). In order to make a ribbon with two half rings (bottom right), the E -field direction needs to be changed shortly after the coalescence.

time, the two droplets start to approach one another due to the combined action of EHD asymmetric flows and the dipole-dipole electrostatic attraction [18]. After a short time, the droplets contact each other, as shown in the second panel in Fig. 4. Eventually, the droplets electro-coalesce. If the E -field direction remains constant, the two ribbons are carried by the EHD flows of the merged droplet towards the electric equator of the droplet forming a two-striped ribbon (top right panel in Fig. 4). However, if the E -field direction is changed right after the coalescence, a ribbon composed of two half rings with different materials can be made (bottom right panel in Fig. 4).

Merging two droplets decreases the total surface area of the interface with the outer liquid. Thus, when the particle concentration on each droplet is adequately high, a jammed shell, i.e., a shell composed of closely packed particles; can be formed by electro-coalescence (similarly as for merged droplets in Fig. 4). In a merged droplet, the particles have practically no freedom to move, hence cannot diffuse within the layer. In our previous report [4] we demonstrated an approach to fabricating a range of jammed capsules, including Janus and patchy capsules. The capsule can be made to be non-spherical (e.g., ellipsoidal or dumbbell-like) and its shape is determined by the particle surface coverage of the droplets before their coalescence [4]. If the surface particles are densely packed and jammed, the capsule maintains its shape, as long as the force exerted on the capsule (e.g., by applying high electric field) overcomes the elastic stress of the capsule. The capsules reported in [4] were made of shells composed of either non-conductive or weakly-conductive particles. Here, we present a capsule comprising both non-conductive (polyethylene) and conductive (silver-coated glass) particles within a monolayer shell.

As shown in Fig. 5, the process of fabrication of an arrested spherical or non-spherical capsule involves two steps, namely electro-coalescence and 'electro-

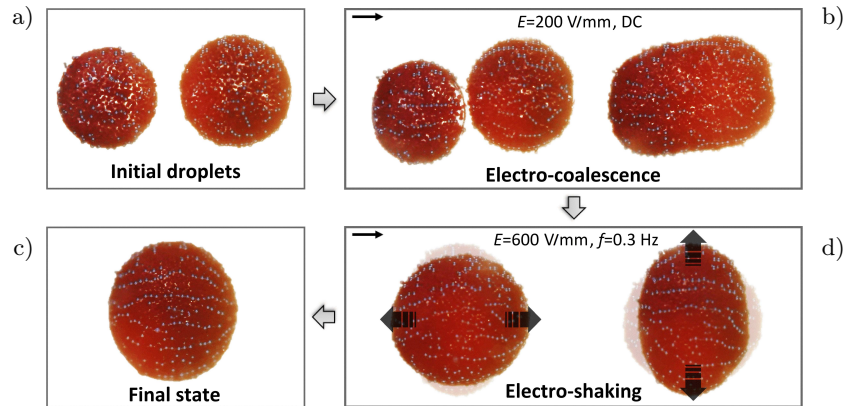


FIG. 5. The process of fabrication of an arrested non-spherical capsule with conductive chains. The process involves two steps, namely electro-coalescence and ‘electro-shaking’. a) The surface particles are dispersed randomly. b) After application of a DC E -field of around 200 V/mm the particles on each droplet move towards electric equators and at the same time the droplets approach one another. It takes just few seconds for the droplets to electro-coalesce and form a prolate-like arrested capsule. c) The coalesced droplet is electro-shaken at $E = 600$ V/mm and $f = 0.3$ Hz. This process aids conductive particles to move, re-locate and form conductive chains. After many electro-shaking cycles the electric field is turned off. d) The resulting arrested capsule acquires an oblate-like shape. Since the particles are jammed, the conductive chains stay at their positions permanently, as long as $E < E_c$. During electro-coalescence and ‘electro-shaking’, the E -field is in horizontal direction.

shaking’. The initial two droplets, with surface particles distributed randomly, are shown in Fig. 5a. The concentration of the particles on each droplet has to be sufficiently high to obtain an arrested capsule after electro-coalescence. The electro-coalescence is performed at a DC E -field of around 200 V/mm. The right panel of Fig. 5b shows the resulting electro-coalesced arrested capsule. The capsule acquires a prolate-like shape and the shape is maintained as long as $E \leq E_c$. The critical electric field strength $(E_c)_\tau$ is a strength at which the electric force exerted on a capsule has the same magnitude as the elastic stress of the capsule (here around 350 V/mm). Above that value the capsule starts to deform and may eventually acquire an oblate shape. The conductive particles are now trapped and cannot re-locate since all of the surface particles are jammed. We ‘electro-shake’ the droplet in order to allow the conductive particles to move on the surface of a droplet and eventually assemble into chains. The details of this method were explained in our previous publication [13]. In short, a slowly alternating electric field (here $f = 0.3$ Hz) compresses and elongates the droplets cyclically (see Fig. 5c). This can be done at $E \gg E_c$, here at $E = 600$ V/mm. After around 30 s of electro-shaking the electric field is turned off exactly when the droplet is the most compressed. The droplet elastically relaxes until the sur-

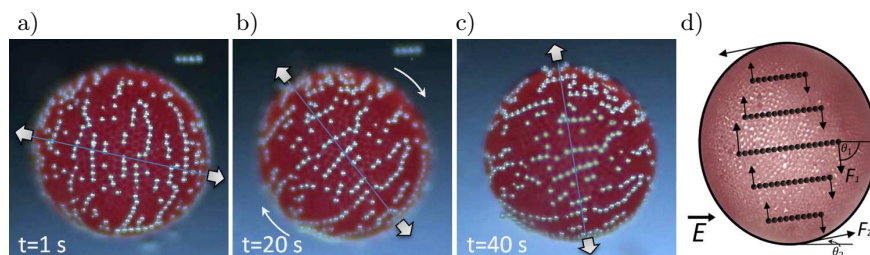


FIG. 6. a)–c) Alignment of a capsule subjected to an applied E -field. The capsule consists of red PE particles and of silver conductive particles that form short chains. In the presence of an external AC E -field (100 Hz), the capsule undergoes electro-orientation and changes its configuration from an initially non-axisymmetric towards an axisymmetric, i.e., it aligns itself with the dipolar chains oriented roughly along the E -field lines. The direction of the rotation here is clockwise, defined by the initial direction of the deviation from the non-axisymmetric configuration. As the droplet rotates, the repartition of the conductive particles remains still, since the particles within the monolayered shell are jammed. The size of the capsule is about 1.5 mm. d) Schematic representation of a capsule with conductive chains and force vectors F_1 and F_2 due to electric torques induced on chains and the capsule, respectively. The direction of the E -field is horizontal, in all panels.

face particles jams. The resulting oblate-shape droplet with aligned conductive chains is shown in Fig. 5d. Once the oblate-shape jammed capsule is formed, the conductive chains stay at their positions permanently, as long as $E \leq E_c$. The droplet, with a jammed capsule formed on its surface, behaves as a rigid body, unless the particles unjam, e.g., due to application of high E -fields.

Figure 6 shows a slightly non-spherical capsule, which was intentionally rotated by around 80° (by mechanical means) in respect to its original orientation (i.e., just after the capsule's formation). Its longest axis is now nearly parallel to the direction of the E -field. In the presence of a moderate external AC E -field (100 Hz, 300 V/mm), the capsule keeps its shape (such magnitude of the electric force acting on the capsule is too weak to induce any observable viscoelastic deformation) and undergoes electro-orientation changing its configuration from initially approximately non-axisymmetric towards axisymmetric, i.e., it aligns itself with the dipolar chains oriented roughly along the E -field lines. The direction of the rotation (clockwise or counter-clockwise) depends on the initial direction of the deviation from the non-axisymmetric configuration. The rotation dynamics is primarily dependent on the viscosity of the external phase, i.e., lowering the viscosity of castor oil 10 times would result in reducing the time of rotation to about 4 s.

For a non-spherical and dielectrically homogenous capsule (comprising, e.g., PE particles), the dipole moment aligns along its longest axis. This, in turn, determines the alignment of the particles in the E -field, via electro-rotation. Interestingly, here (Fig. 6) the alignment of the capsule does not occur with its

longest principal axis oriented along the E -field. At the AC E -field the conductive chains seems to define the direction of alignment. The exact prediction of the capsule's preferred orientation seems to be a non-trivial task, since such a system contains four different media: internal oil, dispersing oil with different dielectric properties, a non-conductive main part of the shell and finally conductive chains. By simplifying the system to three phases (only one type of liquid) we can apply the following reasoning. Each dipolar chain that is not aligned along the E -field direction, experiences an induced torque with a force vector (e.g., F_1 in Fig. 6d) due to the external electric field. The torque tends to align the dipolar chain towards the direction of the E -field. The magnitude of the electric torque is related to: (i) the strength of the electric dipoles, thus it depends on the length of a chain and its polarizability; (ii) the electric field strength; and (iii) the cosine of the angle formed between the direction of the force vector and the electric field lines. The total torque of dipolar chains is balanced by the electric torque (with a force vector F_2) that a non-spherical capsules experiences. This balance is achieved at a certain orientation of the capsule and, in respect to the angle θ_2 , it is determined by induced electric dipoles of both the dipolar chains and the capsule, as following:

$$\theta_2 = \tan^{-1} \left(\frac{p_{dip}}{p_{cap}} \right).$$

Thus, if $p_{dip} \gg p_{cap}$ the angle $\theta_2 \rightarrow 90^\circ$, and the capsule attains the axisymmetric configuration, i.e., it aligns itself with the dipolar chains oriented roughly along the E -field lines.

It would be interesting to investigate the orientation-spectrum of capsules (composed of similar complex shells) with varied frequency of applied E -fields and conductivities of the three media. We foresee that with adequately chosen material and E -fields it will be possible to electro-switch the orientation of a capsule, changing its configuration from non-axisymmetric to axisymmetric, and vice-versa. This phenomenon could potentially be of use in, e.g., passive display technology.

2.5. Particles binding at the droplet interface

As a final remark, we discuss the importance of an appropriate selection of oils and particles. There are many mechanisms for transporting particles onto the surface of the droplet, and they utilize either gravity [22], mechanical shearing [23], spontaneous assembly [24] or hydrodynamic delivery [25]. Once particles are brought to the interface, they should preferably be strongly bound to it. The binding energy, or the energy required to remove a particle from the interface with a surface tension γ is given as [26]:

$$(2.7) \quad E_b \propto a^2 \gamma (1 \pm \cos \theta)^2,$$

where a is the particle radius, θ is the contact angle and the sign inside the bracket is negative for a transfer of the particle into the droplet, and positive for removal into the outer surrounding liquid. The particles are bound to the interface most strongly when the contact angle is 90° . This condition is difficult to achieve because typically particles comprising a single material exhibit different contact angles of the two immiscible liquids. For example, polystyrene particles may have much higher affinity to the castor oil than to the silicone oil (Fig. 7a). Gentle mechanical stirring, EHD flows or any viscous drag due to, e.g., the flow of the droplet; may cause de-attachment of the particles from the interface (Fig. 7c).

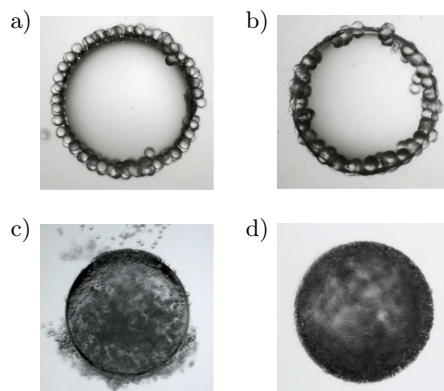


FIG. 7. The importance of an appropriate selection of oils and particles. A silicone oil with pure (a, c) and surface modified (b, d) PS particles with radii of 140 and 40 μm in panels (a, b) and (c, d), respectively. The droplets are immersed in castor oil. The pure PS particles are very weakly bound to the interface. They diffuse to the castor oil phase to which they have much greater affinity. Gentle deformation or displacement of the droplet caused the non-modified particles to easily deattach from the surface (c). Surface modification of PS particles resulted in change of the contact angle, thus the modified PS particles bind strongly to the interface (d). In (a) and (b) particles form a ribbon view along the electric field lines.

Modification of the surface chemistry of the particles may balance the wettability of the particles by the liquids. In our experiments we used an acrylate polymer surface modifier (FluoroPELTM PFC 502AFA, Cytonix, USA) diluted with fluorinated fluid (HFE7100, 3MTM, USA) to improve the affinity of PS particles towards castor oil. PS were added to the mixture and stirred for 20 min at approx. 50°C . The solvent was then removed by using a rotary evaporator. Subsequently, the PS particles were placed in silicone oil and sonicated to avoid aggregations. The modification resulted in the change of the contact angle (compare Fig. 7a with Fig. 7b) and the particles are hence more strongly bound to the interface, as shown in Figs. 7b and Fig. 7d, respectively. Another way to assure the particle stability would be to use heterogonous colloidal particles, e.g., Janus particles, in which two hemispheres are composed of different materials

that possess the right affinity to both liquid phases. The equilibrium contact angle for such particles is nearly 90° [27].

3. Conclusions

We discussed the general behavior of oil droplets subjected to electric fields and showed an example of the E -field-induced deformation of a droplet of silicone oil immersed in castor oil. We also detailed the deformation dynamics of the droplet. We found that the characteristic deformation time is proportional to E^{-2} , and has the offset defined by the value of Maxwell–Wagner time (charge built-up time). The latter is an important parameter that sets the critical frequency of E -field above which the accumulation of charges on a surface of a droplet will be suppressed. For the oil-oil system presented here, we found the critical frequency to be of around 0.8 Hz. Thus, only slowly changing E -field (below 0.8 Hz) can be used to induce EHD liquid flows. We observed the EHD flow patterns by tracing particles and found the direction of flow to be from the electric poles towards the electric equator.

We further described the phenomenon of induced liquid flows by E -fields and that electro-coalescence can be used to manipulate particles on a surface of a droplet. We have provided examples of three different surface structures, including a two-striped ribbon and a ribbon that is composed of two half rings of different materials; and a patchy capsule composed of both non-conductive polymeric particles and conductive silver coated particles. The assembled particles can possibly be interlocked, for example, by sintering or curing. Then, such an interlocked object could be removed from dispersion, rinsed and dried for use in other systems. In addition, the structures can be transformed into solid patchy particles if the inner liquid phase is solidified, for example, by UV curing.

We also demonstrated electro-orientation of a non-spherical patchy capsule composed of a non-conductive shell with several integrated conductive chains. The conductive chains were pre-aligned in direction perpendicular to the elongation axis. In presence of an AC E -field, the capsule aligned itself with the dipolar chains oriented along the E -field lines. A non-spherical, but dielectrically homogenous capsule aligns with its longest axis along the E -field lines. By adding conductive chains we changed a distribution of charges within a shell and the direction of a net dipole.

The capillary binding of particles to a surface of a droplet is related to their wettability and the contact angle of the oil-oil interface at the particles. By coating PS particles with acrylate polymers we modified particles' surface properties and changed their wettability. More specifically, due to the modification we changed the contact angle (approaching optimal value of 90°) by lowering the affinity of particles towards castor oil in favor of silicone oil. This resulted

in an increase of the free energy of adsorption and consequently prevented from detachment of particles from the surface of a droplet. The modified particles held strongly to the interface even if exposed to strong liquid flows.

Acknowledgment

Z. Rozynek acknowledges the financial support from the Foundation for Polish Science through Homing Plus programme. We wish to thank to K. J. Måløy for help in revising the manuscript and for his kind agreement to perform part of the experimental work at the Department of Physics at the University of Oslo. A. Mikkelsen is acknowledged for assistance in collecting data in Fig. 2. We also thank A. Mikkelsen, J. O. Fossum and P. Dommersnes for fruitful discussions. P. Garstecki acknowledges support within the European Research Council Starting Grant 279647.

References

1. G. TAYLOR, *Studies in Electrohydrodynamics. I. The Circulation Produced in a Drop by Electrical Field*, Proc. R. Soc. A Math. Phys. Eng. Sci., **291**, 159–166, 1966.
2. P. DOMMERSNES, Z. ROZYNEK, A. MIKKELSEN, R. CASTBERG, K. KJERSTAD, K. HERSVIK, J.O. FOSSUM, *Active structuring of colloidal armour on liquid drops*, Nat. Commun., **4**, 2066, 2013.
3. M. OURIEMI, P.M. VLAHOVSKA, *Electrohydrodynamics of particle-covered drops*, J. Fluid Mech., **751**, 106–120, 2014.
4. Z. ROZYNEK, A. MIKKELSEN, P. DOMMERSNES, J.O. FOSSUM, *Electroformation of Janus and patchy capsules*, Nat. Commun., **5**, 3945, 2014.
5. L. HONG, A. CACCIUTO, E. LUIJTEN, S. GRANICK, *Clusters of amphiphilic colloidal spheres*, Langmuir, **24**, 621–625, 2008.
6. Z. LI, M. XIAO, J. WANG, T. NGAI, *Pure protein scaffolds from pickering high internal phase emulsion template*, Macromol. Rapid Commun., **34**, 169–174, 2013.
7. G.R. YI, D.J. PINE, S. SACANNA, *Recent progress on patchy colloids and their self-assembly*, J. Phys. Condens. Mat., **25**, 193101, 2013.
8. F. PORTA, A. KROS, *Colloidosomes as single implantable beads for the in vivo delivery of hydrophobic drugs*, Part. Part. Syst. Char., **30**, 606–613, 2013.
9. P.H.R. KEEN, N.K.H. SLATER, A.F. ROUTH, *Encapsulation of amylase in colloidosomes*, Langmuir, **30**, 1939–1948, 2014.
10. H.N. YOW, A.F. ROUTH, *Release profiles of encapsulated actives from colloidosomes sintered for various durations*, Langmuir, **25**, 159–166, 2009.
11. Y. WU, Z. WU, X. LIN, Q. HE, J. LI, *Autonomous movement of controllable assembled Janus capsule motors*, ACS Nano, **6**, 10910–10916, 2012.

12. A. WALTHER, A.H.E. MUELLER, *Janus particles: synthesis, self-assembly, physical properties, and applications*, Chem. Rev., **113**, 5194–5261, 2013.
13. 13. Z. ROZYNEK, P. DOMMERSNES, A. MIKKELSEN, L. MICHELS, J.O. FOSSUM, *Electrohydrodynamic controlled assembly and fracturing of thin colloidal particle films confined at drop interfaces*, Eur. Phys. J. Spec. Top., **223**, 1859–1867, 2014.
14. 14. O.J. CAYRE, J. HITCHCOCK, M.S. MANGA, S. FINCHAM, A. SIMOES, R.A. WILLIAMS, S. BIGGS, *PH-responsive colloidosomes and their use for controlling release*, Soft Matter, **8**, 4717–4724, 2012.
15. A. GIACOMETTI, F. LADO, J. LARGO, G. PASTORE, F. SCIORTINO, *Effects of patch size and number within a simple model of patchy colloids*, J. Chem. Phys., **132**, 174110, 2010.
16. H. REZVANTALAB, S. SHOJAEI-ZADEH, *Designing patchy particles for optimum interfacial activity*, Phys. Chem. Chem. Phys., **16**, 8283–8293, 2014.
17. D.A. SAVILLE, *Electrohydrodynamics: The Taylor–Melcher leaky dielectric model*, Annu. Rev. Fluid Mech., **29**, 27–64, 1997.
18. J.C. BAYGENTS, N.J. RIVETTE, H.A. STONE, *Electrohydrodynamic deformation and interaction of drop pairs*, J. Fluid Mech., **368**, 359–375, 1998.
19. T.B. JONES, *Electromechanics of Particles*, Cambridge University Press, New York 1995.
20. P.F. SALIPANTE, P.M. VLAHOVSKA, *Electrohydrodynamics of drops in strong uniform DC electric fields*, Phys. Fluids, **22**, 2010.
21. G. QUINCKE, *Ueber Rotationen im constanten elektrischen Felde*, Annalen der Physik, **295**, 417–486, 1896.
22. 22. S. NUDURUPATI, M. JANJUA, N. AUBRY, P. SINGH, *Concentrating particles on drop surfaces using external electric fields*, Electrophoresis, **29**, 1164–1172, 2008.
23. K.L. THOMPSON, S.P. ARMES, D.W. YORK, *Preparation of pickering emulsions and colloidosomes with relatively narrow size distributions by stirred cell membrane emulsification*, Langmuir, **27**, 2357–2363, 2011.
24. M.F. HSU, M.G. NIKOLAIDES, A.D. DINSMORE, A.R. BAUSCH, V.D. GORDON, X. CHEN, J.W. HUTCHINSON, D.A. WEITZ, *Self-assembled shells composed of colloidal particles: fabrication and characterization*, Langmuir, **21**, 2963–2970, 2005.
25. A.B. SUBRAMANIAM, M. ABKARIAN, H.A. STONE, *Controlled assembly of jammed colloidal shells on fluid droplets*, Nat. Mater., **4**, 553–556, 2005.
26. 26. S. LEVINE, B.D. BOWEN, S.J. PARTRIDGE, *Stabilization of emulsions by fine particles I. Partitioning of particles between continuous phase and oil/water interface*, Colloids and Surfaces, **38**, 325–343, 1989.
27. R. AVEYARD, B.P. BINKS, J.H. CLINT, *Emulsions stabilised solely by colloidal particles*, Adv. Colloid Interface Sci., **100**, 503–546, 2003.

Received March 27, 2015; revised version June 9, 2015.